Regular Paper for J. Biochem. Biochemistry (Protein structure)

Crystal Structure of Serine Dehydrogenase from *Escherichia coli*: Important role of the C-terminal region for closed-complex formation

Ryuji Yamazawa, Yoshitaka Nakajima, Karin Mushiake, Tadashi Yoshimoto[‡] and Kiyoshi Ito*

Graduate School of Biomedical Sciences, Nagasaki University, 1-14 Bunkyo-machi, Nagasaki 852-8521, Japan

Running title: Crystal structure of serine dehydrogenase.

*Corresponding author: Kiyoshi Ito, k-ito@nagasaki-u.ac.jp, Tel: +81-95-819-2436, Fax: +81-95-819-2478

Abbreviations: SerDH, Serine dehydrogenase; SDR, short-chain dehydrogenase/reductase; PfHBDH, D-3-hydroxybutyrate dehydrogenase from *Pseudomonas fragi*; rms, root mean square; MIR, molecular isomorphous replacement method

SUMMARY

Serine dehydrogenase from *Escherichia coli* is a homotetrameric enzyme belonging to the short-chain dehydrogenase/reductase (SDR) family. This enzyme catalyzes the $NADP^+$-dependent oxidation of serine to 2-aminomalonate semialdehyde. The enzyme shows a stereospecificity for β-(3*S*)-hydroxy acid as a substrate; however, no stereospecificity was observed at the α-carbon.

The structures of the ligand-free SerDH and SerDH-$NADP^+$-phosphate complex were determined at 1.9 Å and 2.7 Å resolution, respectively. The overall structure, including the catalytic tetrad of Asn106, Ser134, Tyr147, and Lys151, shows obvious relationships with other members of the SDR family. The structure of the substrate-binding loop and that of the C-terminal region were disordered in the ligand-free enzyme, whereas these structures were clearly defined in the SerDH-$NADP^+$ complex as a closed form. Interestingly, the C-terminal region was protruded from the main body and it formed an antiparallel β-sheet with another C-terminal region on the subunit that is diagonally opposite that in the tetramer. It is revealed that the C-terminal region possesses the important roles in substrate binding through the stabilization of the substrate-binding loop in the closed form complex. The roles of the C-terminal region along with those of the residues involved in substrate recognition were studied by site-directed mutagenesis.

INTRODUCTION

Serine dehydrogenase (SerDH: EC 1.1.1.276) from *Escherichia coli* is an enzyme that reversibly oxidizes serine to 2-amino-malonate semialdehyde using $NADP^+$ as a cosubstrate. The enzyme shows high levels of activity toward L-(2*S*)-serine, D-(2*R*)-serine, D-(2*R*, 3*S*)-threonine, and L-(2*S*, 3*S*)-allo-threonine as substrates: L-allo-threonine is the best substrate for SerDH (*1*). Therefore, SerDH is also known as L-allo-threonine dehydrogenase. SerDH oxidizes 3*S*-isomers of threonine to respective 2-amino-acetoacetate isomers. The products of the SerDH-catalyzed reaction, 2-amino-malonate semialdehyde and 2-amino-acetoacetate would be spontaneously converted into 2-amino-acetoaldehyde and aminoacetone, respectively. The details of the physiological roles of SerDH have not been clarified. However, Kim and co-workers recently reported that this enzyme is involved in the Rut pathway for pyrimidine degradation through an overlapping function with RutE (*2*).

E. coli SerDH is a tetrameric enzyme containing four identical subunits. The monomer consists of 248 amino acid residues, and the subunit molecular weight was 27,249. SerDH belongs to the short-chain dehydrogenase/reductase (SDR) family (*1*). More than 79,000 primary sequences of SDR enzymes are annotated in the sequence databases if the sequences of species variants are included. The SDR family enzymes act on a great variety of compounds and are classified into several EC classes from oxidoreductases to isomerases. Moreover, among the subgroup of oxidoreductases to which most of the enzymes belong, diverse substrate specificities are found to act on a range of compounds: steroids, aliphatic alcohols, sugars, and so on. The diversity of the SDR family might be in the same range as that of the CYP P450 family (*3*). The amino acid sequence identity among SDRs is relatively low, roughly 15-30%. However, the

three-dimensional structures of the SDR family enzymes have similar architectures, except for the substrate-binding loop region (*4*). Based on the functional assignments of the co-substrate binding motif, the SDR family was divided into five subfamilies: classical, extended, intermediate, divergent, and complex (*5*). The catalytic tetrad of Asn-Ser-Tyr-Lys is conserved in most of the oxidoreductases in this family (*6*). Since some particular SDR members could be drug targets and some could be useful as enzyme reagents in organic synthesis or chemistry, it is very important to understand the strategies used to recognize substrates in SDR enzymes. One of the striking features of SDR enzymes, mainly for the classical type, is a large conformational change upon substrate or cosubstrate binding (*3*, *4*). Most of the variable region of the substrate-binding loop moves to cover the substrate for catalysis.

We determined the crystal structures of D-3-hydroxybutyrate dehydrogenase from *Pseudomonas fragi* (PfHBDH) and 7α-hydroxysteroid dehydrogenase from *Escherichia coli* in this family, and clarified their substrate-recognition mechanisms (*7*-*11*). PfHBDH catalyzes the reversible oxidation reaction from 3-hydroxybutyrate to acetoacetate using NAD^+ as a cosubstrate, and shows a strict stereospecificity to the D-enantiomer of 3-hydroxybutyrate. Stringent stereo-specificity was achieved through the recognition of the carboxyl group and the methyl group of the substrate. The PfHBDH acted on L-threonine, which has a similar structure to D-3-hydroxybutyrate. In order to understand the substrate recognition mechanism of SDR, we searched for an SDR enzyme that can act specifically on threonine-related compounds, and found the *E. coli* SerDH.

In this study, we investigated the substrate specificity of SerDH and determined the crystal structure of the ligand-free enzyme and its complex with $NADP^+$. On the basis of these

structures, along with the site-directed mutagenesis experiments, we discussed the substrate recognition mechanism and the roles of the C-terminal region of *E. coli* SerDH.

MATERIALS AND METHODS

Materials

Restriction endonucleases and other DNA modification enzymes were purchased from TaKaRa Bio Inc. (Shiga, Japan). The oligonucleotide primers were synthesized by Genenet Co., Ltd. (Fukuoka, Japan). The BigDye Terminator v1.1 cycle sequencing kit and other reagents used for sequencing were obtained from Life Technologies Co. (Carlsbad, CA). Polyethylene glycol 400 (PEG400), isopropyl-β-thiogalactopyranoside (IPTG), L-(2*S*)-serine, L-(2*S*, 3*R*)-threonine, D-(2*R*, 3*S*)-threonine, malonic acid, and $NADP^+$ were purchased from Nacalai Tesque Inc. (Kyoto, Japan). D-(2*R*)-serine, D-(2*R*, 3*S*)-threonine, L-(2*S*, 3*S*)-allothreonine, D-(2*R*, 3*R*)-threonine, (±)-1, 2-butanediol, (±)-1, 3-butanediol, and 1, 4-butanediol were purchased from Wako Pure Chemical Industries (Osaka, Japan). 1-aminopropanol and 1-aminobutanol were purchased from Kanto Chemical Co., Inc. (Ibaraki, Japan).

Bacterial strains and plasmids

E. coli XL1Blue (Stratagene, La Jolla, CA) was used for DNA manipulation and protein expression. pGEM-T Easy (Promega) was used for cloning the PCR products, and pQE30 (Qiagen, Hiden, Germany) and pKK223-3 (Pharmacia, Uppsala, Sweden) were used to express the recombinant enzymes.

Cloning of the SerDH gene

A DNA fragment coding for SerDH was amplified from the *E. coli* XL1Blue genomic DNA by using the primers based on a previously reported sequence. The chromosomal DNAs of *E.*

coli XL1-Blue were prepared by standard protocols (*12*). The PCR reaction was carried out using the primer set of EcSDH1s and EcSDH2a (Table 1). The amplified fragment was cloned into pGEM-T Easy, and the nucleotide sequence was determined by using the ABI Prism 3100 Avant Genetic Analyzer using the BigDye Terminator v1.1 cycle sequencing kit. The plasmid was digested with EcoRI and HindIII, and the resultant DNA fragment of 0.75 kb containing the SerDH structural gene was ligated into the same restriction sites of pKK223-3 to produce the expression plasmid pEcSerDH_X1.

Expression and purification of the wild-type SerDH

The wild-type enzyme was expressed in *E. coli* XL1Blue transformed with pEcSerDH_X1. The transformants were aerobically cultivated in 20 L N-broth containing 50 μg/mL ampicillin at 37˚C for 16 h using a jar fermenter (MBS, Yamaguchi, Japan). The cells were suspended in 20 mM Tris-HCl buffer (pH 7.5) and were disrupted with glass beads in a Dyno-Mill (HITACHI, Tokyo, Japan). The cell lysate was centrifuged at 15,000*g* for 30 min in order to remove cell debris. To remove the nucleic acids, 2% (w/v) protamine sulfate was added to the supernatant in a dropwise fashion at a ratio of 17 mg per g of wet weight. After centrifugation, ammonium sulfate was added to the supernatant at 40% saturation, and the solution was applied to a Toyopearl Butyl-650C column equilibrated with 20 mM Tris-HCl buffer (pH 7.5) containing 40% saturated ammonium sulfate. Enzymes were eluted using a decreasing linear gradient of ammonium sulfate concentration from 40 to 0% saturation. Active fractions were combined and dialyzed against 20 mM Tris-HCl (pH 7.5). The enzyme was purified using a Toyopearl DEAE-650C column using an increasing linear gradient from 0 to 500 mM NaCl.

The purified enzyme was dialyzed against 5 mM Tris-HCl buffer (pH 7.5). The protein solution was concentrated to 24 mg/ml using Centricon YM-3 (Millipore, Bedford MA) and stored at -80˚C.

Enzyme activity assay and kinetic analysis

An enzyme activity assay was carried out using the reaction mixture containing enzyme, 100 mM substrate, and 1 mM $NADP^+$ in 100 mM Tris-HCl buffer (pH 8.5). After 2 min pre-incubation at 30˚C, the reaction was started by adding 0.05 ml of enzyme solution. The reaction was monitored by measuring absorbance at 340 nm for 2 min. One unit of enzyme activity was defined as the amount of enzyme that reduces 1 μmol of $NADP^+$ per minute under the above conditions.

The kinetic parameters were estimated from a Lineweaver-Burk plot. The K_M value was determined with various concentrations of the substrate (1-300 mM) in the presence of 2 mM $NADP^+$. The K_M value for $NADP^+$ was determined with various concentrations of $NADP^+$ (0.1-2 mM) in the presence of 200 mM L-serine as a substrate.

Crystallization and data collection

Crystals of the ligand-free enzyme were grown by the hanging-drop vapor diffusion method at 20˚C using the wild-type enzyme solution dissolved in 5 mM Tris-HCl buffer (pH 7.5). Initial screening was performed using commercially available kits: Cryo I and II, and Wizard I, II, and III screening kits (Emerald Biostructures, Bainbridge Island, WA) as well as the PEG/ION screening kit (Hampton Research Inc. Aliso Viejo, CA). Several forms of crystals were obtained,

and one of the more promising crystallized conditions was optimized. A droplet (1 μL) of 26.5 mg/ml enzyme solution mixed with the same amount of reservoir solution was equilibrated against 500 μl reservoir solution [30-36% (v/v) PEG 400, 100 mM $MgCl_2$, and 100 mM HEPES-Na buffer (pH 7.6)] to give SerDH crystals. After 3 days, hexagonal-column-shaped crystals grew to average dimensions of 0.05 x 0.05 x 0.3 mm^3. The crystallized condition for the enzyme complexed with $NADP^+$ was rescreened under the same conditions using the enzyme solution in 50 mM Tris-HCl buffer (pH 8.5) containing 10 mM $NADP^+$. A droplet (2 μL) of 22.5 mg/ml enzyme solution mixed with the same volume of reservoir solution was equilibrated against 500 μL reservoir solution [1.9-2.0 M Na/K_2 phosphate, 50-100 mM $LiSO_4$, and 100 mM Na acetate buffer (pH 4.5)] to give crystals of the enzyme-$NDAP^+$ complex. Stock solution of 4 M Na/K_2 phosphate was prepared by mixing 1.6 M NaH_2PO_4 and 2.4 M K_2HPO_4. After several days, hexagonal-column-shaped crystals grew to average dimensions of 0.1 x 0.1 x 0.3 mm^3.

X-ray diffraction data from the ligand-free crystal were collected using a wavelength of 1.000 Å from the synchrotron-radiation source at the Photon Factory BL17A station with an ADSC Quantum 270 detector system (Tsukuba, Japan). The data from the crystal of enzyme complexed with $NADP^+$ were collected using Cu*K*α generated by RIGAKU Micromax007 HF with an R-AXIS IV^{++} detector system. For data collection under cryogenic conditions, a crystal of the enzyme complexed with $NADP^+$ was soaked for a few seconds in prepared solution containing 20% (w/v) sucrose, 5% (v/v) glycerol, 2.1 M Na/K_2 phosphate, 100 mM $MgCl_2$, and 100 mM Na acetate buffer (pH 4.5). Crystals were mounted in a nylon loop and flash-cooled in a nitrogen stream at -173˚C. All data sets were processed and scaled using the program HKL2000 (*13*). X-ray data collection statistics are summarized in Table 2. The atomic

coordinates of the ligand-free enzyme and the enzyme complexed with $NADP^+$ (PDB code: 3ASU and 3ASV) have been deposited in the Worldwide Protein Data Bank (wwPDB; http://www.wwpdb.org) and in the Protein Data Bank Japan at the Institute for Protein Research, Osaka University (PDBj; http://www.pdbj.org/).

Structure determination and refinement

The crystal of ligand-free enzyme belonged to the Laue group *P*321 with the following unit-cell parameters: $a = b = 66.79$, $c = 175.9$ Å, and $\gamma = 120°$. Assuming two subunits of tetramer in the asymmetric unit, the Matthews coefficient V_M value was calculated to be 2.07 $Å^3$ Da^{-1}, indicating a solvent content of approximately 41% in the unit cell. The initial phase was determined by the molecular replacement (MIR) method using coordinates of short-chain dehydrogenase from *Pseudomonas aeruginosa* (PDB code: 2NWQ), which shows 51% of sequence identity with the *E. coli* SerDH, as an search model by the program PHASER in the CCP4 program suite (*14*). The solution was obtained assuming the crystal belongs to the space group $P3_121$. The structure of ligand-free enzyme was refined by simulated annealing and energy minimization with the program CNS (*15*) using the data from 20 to 1.9 Å resolution. The structure was scrutinized by inspecting the composite omit map using the program CNS (*15*). After several rounds of refinement and manual rebuilding, water molecules were picked up on the basis of the peak height and the distance criteria from the difference map using the program COOT (*16*). Furthermore, model building and refinement cycles resulted in an *R*-factor of 20.0% and R_{free} of 23.0% using 36,558 reflections from 20 to 1.9 Å resolution.

The crystal of the enzyme complexed with $NADP^+$ belonged to the space group $P6_4$ with unit-cell parameters $a = b = 113.9$, $c = 197.5$ Å, and $\gamma = 120°$. One tetramer and one dimer of a tetramer were found in the asymmetric unit from the solution of the MIR method using coordinates of the ligand-free enzyme as a search model by the program PHASER in the CCP4 program suite (*14*). From the results of model building with the program COOT (*16*) and refinement with the program CNS (*15*), the *R*-factor and R_{free} decreased to 19.4% and 27.2% using 39,711 reflections from 20 to 2.7 Å resolution. The refinement statistics are summarized in Table 2.

Site-directed mutagenesis

We made specific mutations of Y141A, Y141F, F185A, F185H, F185L, F185W, R189A, and R189K. These mutants were introduced into the gene by the PCR-based megaprimer method, which consisted of two rounds of PCR amplification (*17*). In the first round, one of the flanking primers and the internal mutagenic primer were used to generate a megaprimer. In the second round, another flanking primer (EcSDH2a) and the megaprimer were used to generate the DNA fragment with the desired mutations. In Table 1, the mutagenic and flanking primers are summarized along with the restriction sites to ligate the DNA fragments containing the desired mutations into the plasmid pQE30. PCR conditions consisted of an initial denaturation at 94˚C for 5 min, 25 cycles of denaturation at 94˚C for 30 sec, annealing at 50 or 55˚C for 30 sec, and extension at 72˚C for 1 min, with a final extension at 72˚C for 5 min. Amplified DNA fragments from the first-round PCR were purified from agarose gel by the QIAEX II kit (Qiagen) and used as megaprimers for the second-round PCRs. The second-round PCRs were

carried out under similar conditions as the first round, except for a decrease in the annealing temperature to 47 or 50˚C. The amplified fragments were cloned into the plasmid pGEM-T Easy, and the desired mutations were confirmed by DNA sequencing. The DNA fragments of 0.75 kb containing the specific mutations were excised by BamHI and HindIII digestion and ligated into the same restriction sites of the plasmid pQE30 to produce the expression plasmid for respective mutant enzymes.

The genes having C-terminal deletions (SerDHΔC1, SerDHΔC2, and SerDHΔC7) and specific mutations of the C-terminal residues (R247A, R247K, Q248A, and Q248N) were amplified by PCR by using EcSDH2s and the mutagenic primer containing the stop codon and HindIII restriction sequence. The PCR products were subcloned directly into pQE30 by using the BamHI and HindIII restriction sites.

Expression and purification of the wild-type and mutant enzymes with N-terminal histidine tag

The enzymes were expressed in 2 liters of LB-broth containing 100 mg/L ampicillin at 37˚C in *E. coli* XL1Blue transformed with pQE30-based expression plasmids. The expression was induced by the addition of 0.1 mM IPTG when the OD_{600} reached 0.4-0.5, and the incubation was continued at 37˚C for 4 h. Cells were harvested by centrifugation at 10,000*g* for 10 min at 4˚C and resuspended in 80 mL of 20 mM Tris-HCl buffer (pH 8.0) containing 10 mM imidazole and 0.5 M NaCl. Cell lysate was prepared by using ultrasonic disruptor UD200 (TOMY, Tokyo, Japan), followed by centrifugation at 15,000*g* for 30 min at 4˚C. The crude lysate was applied directly onto a Ni-affinity column (GE Healthcare), and the column was washed with 5 bed

volumes of 20 mM Tris-HCl buffer (pH 8.0) containing 10 mM imidazole and 0.5 M NaCl. The adsorbed enzymes were eluted with 500 mM imidazole dissolved in 20 mM Tris-HCl buffer (pH 8.0) containing 0.5 M NaCl, and the fractions showing significant absorbance at 280 nm were collected. Each collected fraction was dialyzed against 20 mM Tris-HCl buffer (pH 8.0) and applied to a Toyopearl DEAE-650C column. The enzymes were eluted using a linear gradient from 0 to 1 M NaCl in the same buffer. The fractions containing 27 kDa protein on SDS-PAGE analysis were collected and dialyzed against 50 mM Tris-HCl buffer (pH 8.5). The purified enzymes were concentrated to 24 mg/ml using Centricon YM-3 (Millipore) and stored at -80˚C.

RESULTS

Expression and purification of the wild-type and mutant SerDHs

The recombinant wild-type SerDH was efficiently expressed in *E. coli* XL1Blue containing pEcSerDH_X1 and purified to an apparent homogeneity, showing a single band of 27 kDa on SDS-PAGE. The relative activity levels of L-serine, D-serine, D-threonine, and L-allo-threonine were 100, 103, 180, and 290%, respectively. We then determined the kinetic parameters for the purified enzyme using these compounds and confirmed the substrate specificity of that reported by Fujisawa *et al.* (*1*). Since SerDH has no activity toward L-(2*S*, 3*R*)-threonine or D-(2*R*, 3*R*)-allo-threonine, the SerDH likely has a substrate specificity for 3*S*-isomers of 2-amino-carboxylate. However, the stereo isomers at the C2 position (α-carbon) were not clearly distinguished. In order to understand the mechanism underlying the substrate specificity, we tried to solve the crystal structure of *E. coli* SerDH.

Qualities of the structures

Two structures were determined using crystals of the wild-type SerDH and the enzyme complexed with $NADP^+$. The refined model of the ligand-free enzyme contains two subunits of 218 and 218 residues and 245 water molecules in an asymmetric unit with an *R*-factor of 20.0% at 1.9 Å resolution. This model lacked Thr183-Thr204 and Ala241-Gln248 residues, due to insufficient interpretable electron density. The average thermal factors of the main-chain atoms, the side-chain atoms, and the water molecules were 25.1, 30.0, and 33.6 $Å^2$, respectively. Analysis of the stereochemistry with the program PROCHECK (*18*) demonstrated that all of the main-chain atoms fell within the additional allowed region of the Ramachandran plot, with 345

residues (92.5%) in the most-favored region and 28 residues (7.5%) in the additional allowed region.

One tetramer and one dimer of a tetramer were in an asymmetric unit of the enzyme complexed with $NADP^+$. Fourier peaks from $NADP^+$ were found at the active site in each subunit. Additionally, one tetrahedral-shaped peak was located at the active center near the nicotinamide ring of the $NADP^+$. This peak was assigned as a phosphate anion. Briefly, the enzyme complexed with $NADP^+$ was not a binary complex but a ternary complex with $NADP^+$ and phosphate anion. Accordingly, we designate the SerDH complexed with $NADP^+$ and phosphate as ternary complex. The disordered region of the ligand-free enzyme was fixed in the ternary complex, and those structures were determined. The refined model contains six subunits with six $NADP^+$ molecules, six phosphate anions, and 348 water molecules with an *R*-factor of 0.194% at a 2.7 Å resolution. The refinement statistics are summarized in Table 2. Figures were drawn and rendered using the program Open-Source PyMol (http://www.pymol.org).

Overall and subunit structures

The tetramer of the ligand-free enzyme is shown in Fig. 1A and 1B. Two subunits in the asymmetric unit can be mutually superimposed with an rms deviation of 0.26 Å for α-carbons. This is a dimer whose monomers are related to each other by a non-crystallographic 2-fold axis. In the crystal, SerDH tetramer is built by two dimer related by the [100] crystallographic 2-fold axis. The SerDH tetramer shows 222-point group symmetry, and the three perpendicular axes in tetrameric SDR enzymes are conventionally named *P*, *Q*, and *R* (*3*, *5*). The *R*-axis of the three non-crystallographic 2-fold axes coincides with the crystallographic 2-fold axis. In the ternary

complex, one tetramer and one dimer of a tetramer were found in the asymmetric unit, and this dimer formed a tetramer with a symmetrical-related dimer by the *P*-axis coincident with the [001] crystallographic 2-fold axis. The quaternary structure is identical to that in the ligand-free enzyme. Six subunits in the asymmetric unit were superimposed onto each other with rms deviations of 0.25-0.28 Å.

Subunit structures of the ligand-free enzyme and the ternary complex are shown in Fig. 2. The main-chain structure of the ligand-free enzyme is virtually identical to that of the ternary complex with an rms deviation of 0.49 Å except for two factors. One is the disordered region of Thr183-Thr204 and Ala241-Gln248 in the ligand-free enzyme. The other is a conformational change of Thr9-Phe12.

The subunit structure of the SerDH can be divided into three parts: the main body (Met1-Gly182 and Val205-Pro235) of α/β folding patterns including a central β-sheet, typical of the Rossmann-fold motif, the substrate-binding loop (Thr183-Thr204) and the C-terminal region (Val236-Gln248). The common motifs of TGxxxGxG (residues 6-13) for coenzyme binding and NNAG (residues 80-83) for stabilization of the central β-sheet are located at the main body. The subunit of SerDH consists of eight α-helices and nine β-sheets, and has a single α/β domain that comprises a core β-sheet constituted by seven parallel β-strands (β_C, β_B, β_A, β_D, β_E, β_F, and β_G) with three helices (α_C, α_B, and α_G or α_D, α_E, and α_F) on the either side of the sheet, two α-helices (α_1 and α_2) and two β-strands (β_H and β_I) protruding from the main body. These protruding regions, including two α-helices and two β-strands correspond to the disordered regions of Thr183-Thr204 and Ala241-Gln248 in the ligand-free enzyme, respectively. The loop between β_F and α_G, which includes α_1 and α_2, constitutes a substrate-binding loop. The regions

β_A-β_C and α_B-α_D each have a typical Rossmann fold, which is a nucleotide-binding motif that associates an $NADP^+$ or NADPH. The region from β_D to β_I is involved in quaternary structure association and substrate binding. As in the reported SDR enzymes, the regions α_E-α_F and α_H-β_G, including connecting loops, participate in subunit interactions on the *QR* and *PQ* faces, respectively. Additionally, the unique interaction of the C-terminal β-sheets is formed between the β_H on one subunit and the β_I on the other symmetry-related subunit with a 2-fold axis along the *R*-axis.

The $NADP^+$ binding site

The $NADP^+$ binding site and scheme diagram are shown in Fig. 3. The well-defined electron density map as $NADP^+$ was found at the active site. The $NADP^+$ binding mode is similar to those found in the known structures of the SDR family. One of the regions with different conformations between the ligand-free enzyme and the ternary complex was the loop of Thr9-Phe12. These residues are identified in the consensus sequence of Gly7-x-x-x-Gly11-x-Gly13 which is a typical NAD(P)H-binding motif. In the ternary complex, Ala10 and Gly11 were located 2.75 and 2.82 Å away, respectively, from the corresponding positions in the ligand-free enzyme as if opening the $NADP^+$ binding pocket. An adenosine-ribose 5'-diphosphate moiety of $NADP^+$ is accommodated in this part, resulting in the formation of hydrogen bonds with the main-chain NH group of Phe12 and the side-chain hydroxyl group of Thr9. Additionally, this pyrophosphate group forms hydrogen bonds with a side-chain hydroxyl group of Thr183 and a main-chain NH group of Glu184. The adenine moiety of $NADP^+$ is accommodated in the hydrophobic pocket comprised of Arg32, Val55,

Ala82, Leu84, and Thr105. The adenine amino group makes a hydrogen bond with Asp54. The 2'-phosphate group is recognized with Arg32 and Arg33 through hydrogen bonds. The nicotinamide nucleoside moiety is accommodated in the hydrophobic pocket composed of Phe12, Ile132, Pro177, Val180, and Phe185, and the ribose hydroxyl group or the amide group of the nicotinamide ring forms hydrogen bonds with Tyr147 and Lys151, which are catalytic residues, or with a main-chain NH group of Val180, respectively.

The unique C-terminal region

Serine dehydrogenase has a unique C-terminal region compared with other SDR enzymes (Fig. 2). As shown in Fig. 1C and 1D, the C-terminal region forms an anitiparallel β-sheet between subunits A and D or subunits B and C. A stretch of the C-terminal region reaches the substrate-binding loop in the opposite subunit. As a result, Arg247, which is located at the C-terminal in subunit D, forms hydrogen bonds with the main-chain carbonyl groups of Thr200 and Gln202 that are located at the substrate-binding loop in the subunit A. The main-chain NH of Gln248 in the subunit D forms a hydrogen bond with the carbonyl group of Asn203 on the substrate-binding loop of subunit A (Fig. 4). The same interactions between the C-terminal region and the substrate-binding loop were observed in all subunits.

The active-site structure

In the ternary complex, the structure of the substrate-binding loop was determined. Glu184 on the α_1 formed hydrogen bonds with Arg33 and Arg36 at a distance of 2.8 Å, resulting in coverage of the $NADP^+$. In the residues on the α_1, Phe185 is located on the upper side of the

nicotinamide *si*-face, and Val188 and Arg189 forms van der Waals contacts with the main body. Specifically, α_1 makes close contact with the main body and $NADP^+$ in the ternary complex. Meanwhile, no contact was found between the α_2 and the main body, except that an amino group of Lys191 made a hydrogen bond with Asp98 at a distance of 3.1 Å. On the other hands, α_2 interacts with the C-terminal region in the other subunit. This conformation of the substrate-binding loop forms a funnel-shaped pocket on the protein surface, as shown in Fig. 5. As a result, the active site was exposed to solvent, and the phosphate anion and the nicotinamide ring are located at the bottom of this pocket, which is therefore substrate-binding pocket, and it is expected that a substrate would be bound to the bottom of it. The surface of the pocket consisted of Tyr141, Met88 and residues on α_2 of the substrate-binding loop and the C-terminal region of the other subunit. The active site of the ternary complex is shown in Fig. 6. The catalytic tetrad of Asn106, Ser134, Tyr147, and Lys151 is located at typical positions in the SDR family, as shown in Fig. 6. A phosphate anion was bound to the active site by forming hydrogen bonds to Tyr141 and Tyr147. Arg189 on α_1 in the substrate-binding loop formed a hydrogen bond with Tyr141 on the main body at a distance of 3.0 Å. The residues of Tyr141, Phe185, and Arg189 at the active site are completely conserved in the same enzyme from bacteria.

Site-directed mutagenesis

Based on the crystal structure of SerDH and the sequence alignment with the hypothetical serine dehydrogenases (*Shigella dysenteriae*: Swiss-Prot accession no. Q32G40, *Salmonella typhimurium*: P69936, *Burkholderia mallei*: A5TF94, *Aeromonas hydrophila*: A0KFK7, and

Pasteurella multocida: Q9CN62) found by a blast search for DNA databases, we selected Tyr141, Phe185, and Arg189 for mutagenesis as important amino acid residues in substrate recognition. The mutant enzymes of Y141A, Y141F, F185A, F185H, F185L, F185W, R189A, and R189K were constructed. In addition, we also made some mutants with respect to the C-terminal region because it was found to be disordered in the open form and clearly defined in the closed form. To facilitate the purification of these mutant enzymes, a 6x-histidine-tag was introduced to their N-termini using a cloning vector pQE30. The 6x-His tagged wild type (H_6-SerDH) and all the mutants were well expressed to similar levels and these enzymes were efficiently purified by a Ni-chelating column and Toyopearl DEAE column chromatography.

The kinetic parameters of the wild-type and mutant SerDHs are summarized in Table 3. Since similar values were obtained for the wild-type enzyme and the H_6-SerDH, the addition of His-tag had little effect on the enzyme activity. All the mutations introduced into the amino acid residues estimated to be involved in substrate recognition abolished enzyme activity, indicating that these residues were important for enzyme activity.

On the C-terminal deletion mutants, SerDHΔC1, which lacks C-terminal Gln248, showed 54% of the wild-type activity level. However, SerDHΔC2, which lacks Arg247 and Gln248, and SerDHΔC7, which lacks seven C-terminal residues, showed no activity toward L-serine. The mutations at the C-terminal region affected mainly the K_M values, while the effect on k_{cat} values was relatively small. With respect to the K_M values, SerDHΔC1, R247K and R247A showed large increases, approximately 11-, 4.7-, and 17-fold, respectively. The second residue from the C-terminus, Arg247, is well conserved in the sequence alignment. The substitutions of Lys and Ala for this residue decreased the activity toward L-serine to 69% and 20%, respectively,

suggesting that the positive charge of Arg247 may be important for the enzyme activity. On the other hands, the substitution of Asn and Ala for the C-terminal Gln248 had lesser effects on the activity: 80% and 74%, respectively. It is noteworthy that the side chain of residue 248 had little effect on activity, although the truncation of Gln248 greatly decreased activity.

DISCUSSION

The crystal structures of the ligand-free enzyme and the ternary complex were determined for the first time. The strictly conserved residues of the catalytic tetrad in the SDR family are Asn106, Ser134, Tyr147, and Lys151 in the SerDH. In addition, a water molecule is found to form hydrogen bonds with the main-chain carbonyl group and ε-amino group of Lys151, suggesting a proton relay network as proposed by Filling *et al.* (*6*). A large number of three-dimensional structures belonging to the SDR family have been determined by X-ray crystallography (*3*-*6*). To determine the structure of SerDH, we used as a search model the coordinates of 2NWQ, which is registered as a short-chain dehydrogenase of unknown function from *Pseudomonas aeruginosa*. This protein showed 51% sequence identity with SerDH. The structure of 2NWQ, with a 33.4 Z-score from the program DALI (*19*), was superimposed onto that of SerDH at 1.1 Å of the rms deviation. It is likely that this short-chain dehydrogenase from *P. aeruginosa* has a serine dehydrogenase activity, although the structure of the substrate-binding loop was not determined. From the results of the program DALI (*19*), the following structures had high Z-scores of 33.1, 29.3, 27.6, and 27.8, respectively, against the ternary complex: clavulanic acid dehydrogenase complexed with NADPH and clavulanic acid (CAD) from *Streptomyces clavuligerus* (PDB code: 2JAP, *20*), β-keto-acyl-protein reductase complexed with $NADP^+$ (FabG) from *Escherichia coli* (PDB code: 1Q7B, *21*), 17β-hydroxysteroid dehydrogenase (17β-HSDH) complexed with estradiol and $NADP^+$ from *Homo sapience* (PDB code: 1FDT, *22*), and D-3-hydroxybutylate dehydrogenase (PfHBDH) complexed with NAD^+ and L-3-hydroxybutyrate from *Pseudomonas fragi* (PDB code: 2ZTL, *9*). The sequence identities between SerDH and these enzymes are 36, 30, 24, and 23%,

respectively.

In the SDR family, an open-closed conformational change of the substrate-binding loop generally occurs when the substrate is taken into the active site. In the case of PfHBDH, we have determined both open and closed forms (*7*, *9*, *10*); for instance, the substrate-binding loop closes the active site by rotating the main-chain torsion angle around Thr190 and Leu215 as hinges, leading to interactions between the main body and the substrate-binding loop. In addition, rotated Thr190 in the closed form of PfHBDH formed a hydrogen bond with the binding NAD^+ (*9*). Similar interaction was found in the ternary complex of SerDH, which is a hydrogen bond between Thr183 and pyrophosphate moiety of binding $NADP^+$. Above listed structures have been reported as closed forms (*9*, *20-22*) and were superimposed onto the present ternary complex at the corresponding Cα positions within 1 Å of the distance difference by the program GASH (*23*). As shown in Fig. 7, SerDH has a common structure of the main body, and structures characteristic of the substrate-binding loop and the C-terminal region were different from other members of the SDR enzyme that showed high Z-scores. However, the position of the substrate-binding loop was similar to those in the others, although the active site of SerDH is exposed to solvent. Actually, since some residues on the α_1-helix formed hydrogen bonds and van der Waals contacts with $NADP^+$ or residues on the main body, there was no space for the substrate-binding loop to close further more from the present position (Fig. 5). Therefore, we regard this structure of the ternary complex as a closed form.

We discuss the substrate-recognition mechanism on the basis of the active-site structure in the ternary complex. In the SDR family, it is generally known that the catalytic reaction progresses in two steps simultaneously: attraction of a proton on the hydroxyl group by the Tyr residue of

the catalytic triad and hydride transfer from a substrate onto the C4 position of the nicotinamide ring (*3*-*6*). As shown in Fig. 8, the substrate-binding model was built by placing L-allo-threonine into the active site of the closed form on the basis of information accumulated about SDR enzymes to date. Assuming the 3-hydroxy group of L-allo-threonine forms hydrogen bonds with Ser134 and Tyr147 and the 3-hydrogen transfers to the C4 position on the nicotinamide ring as a hydride, it is expected that the α-carboxyl group of L-allo-threonine faces Arg189 at a distance short enough that they can interact with each other. In the ternary complex, Arg189 forms a hydrogen bond with Tyr141. Therefore, the α-carboxyl group of a substrate would be located near Tyr141. The α-carboxyl group is essential for substrate specificity of SerDH. It is likely that Arg189 and Tyr141 are involved in the recognition of the α-carboxyl group of a substrate. In addition, the 3-methyl group was located to a hydrophobic pocket composed of Phe185 and the nicotinamide ring. The SerDH has a strict stereo-specificity for the *S*-isomer at the 3-position of a substrate. Since an access of L-threonine to the active site would be prevented by steric hindrance between the methyl group and $NADP^+$ if the 3*R*-isomer is bound there in the same way, this model agrees with the results of the activity assay. None of the mutant enzymes of R189K, R189A, Y141F, F185A, F185L, F185H, and F185W had any activity toward L-serine. These results indicated that Arg189, Tyr141, and Phe185 are crucial to substrate recognition and the catalytic reaction, and this would be evidences that we have built a suitable model. In our model, no residue was found to specifically interact with the amino group at the 2-position of a substrate. Meanwhile, there is an enough space in the active site to accommodate a substrate with an amino group of both 2*S*- and 2*R*-isomers. Because of this large pocket in the active site, it is considered that SerDH shows no stereoselectivity for the C2 position.

The C-terminal region of the *E. coli* SerDH is very unique, unlike known structures of the reported SDR family. Although this region was disordered in the ligand-free enzyme, however, the structure was fixed and determined in the ternary complex with the closed-form. The stretch of the C-terminal region is involved in the formation of the substrate-binding pocket in the other subunit of the tetramer, indicating the possibility that the C-terminal region is involved in the substrate-recognition mechanism. The activity was lost in SerDHΔC7 in which seven C-terminal residues corresponding to the disordered region in the ligand-free enzyme, suggesting this region has a certain role. Within this region, Arg247 at the second residue from the C-terminus is well conserved. The SerDHΔC2 mutant lost its activity, and the SerDHΔC1 mutant showed a reduced activity. As shown in Fig. 4, the side-chain guanidyl group of Arg247 and the main-chain NH group of Gln248 form hydrogen bonds with the main-chain carbonyl group on the substrate-binding loop at the other subunit. Although some activity remained in the R247K mutant, the deletion of the side chain by the substitution of Ala for Arg247 showed a drastic decrease in the activity. Meanwhile, since Q248N and Q248A mutants show almost the same activity levels, it is unlikely that the side chain of Gln248 is involved in the enzyme activity. Rather, it is indicated that the hydrogen bonds of the side chain on Arg247 and the main chain on Gln248 are crucial to enzyme activity. It is considered that the C-terminal region would stabilize the closed form by keeping the conformation of the substrate-binding loop by these hydrogen bonds. From the results of sequence alignment, Arg251 in the short-chain dehydrogenase from *P. aeruginosa* (PDB code: 2NWQ) corresponds to Arg247 in the SerDH from *E. coli*. In this entry, the structures of three C-terminal residues, Arg251-Ser253, have not been determined, nor has our structure in the ligand-free enzyme. It is considered that a serine

dehydrogenase has a common feature in the C-terminal region involved in the enzyme activity.

We have shown that the formation of the stable closed form of PfHBDH is achieved by substrate binding, not by NAD^+ alone, using kinetic analysis of the mutant enzymes (*7*, *9*). In the case of the closed-form PfHBDH, it is considered that a substrate is maintained by the substrate-binding loop, and the catalytic reaction proceeds at the active site isolated from solvent. In contrast, the active site of SerDH is exposed to solvent even in the closed form. It might be possible that a substrate approaches the active site after forming the closed form by $NADP^+$-binding. Here, we focused on the kinetic parameters of SerDHΔC1 and R247K mutants. Regarding the mutations on the C-terminal regions, the k_{cat} values for both substrates are the same level as those of the H_6-SerDH. However, a large effect was observed on the K_M values. The K_M values for $NADP^+$ stayed at approximately twice those of the H_6-SerDH; however, those for L-serine increased 11-fold and 4.4-fold for the SerDHΔC1 and R247K mutants, respectively. Consequently, these mutations caused little change in the formation of the complex with $NADP^+$. However, the contribution of the C-terminal region to bind L-serine into the active site seems to be significant. Assuming that the C-terminal region would stabilize the closed form by fixing the substrate-binding loop with hydrogen bonds, the closed form of SerDH would be induced by an association of the substrate, not by that of $NADP^+$ as the closed form of PfHBDH. A phosphate salt showed a weak inhibition of SerDH (data not shown). In the ternary complex, although the temperature factors for phosphate anions are comparatively high, there is a possibility that the closed form would be induced by the presence of a phosphate anion at the active site.

In conclusion, the crystal structures of the ligand-free enzyme and the ternary complex

(enzyme complexed with $NADP^+$ and phosphate) were determined. The ternary complex is the closed form of the SDR family. A substrate-recognition mechanism was proposed on the basis of these structures, the substrate-recognition mechanism was proposed. The C-terminal region possesses a unique structure and the role that stabilizes the closed form by fixing the substrate-binding loop in the other subunit through hydrogen bonding.

FOOTNOTES

‡Present address: Department of Life Science, Faculty of Science and Engineering, Setsunan University, 17-8 Ikeda-Nakamachi, Neyagawa, Osaka 572-8508, Japan

ACKNOWLEDGEMENTS

We are grateful to Ms. A. Hisatsugu (Nagasaki University) for her assistance with the enzyme preparation and crystallization. This work was supported in part by the Grant-in-Aid for Scientific Research from Japan Society for the Promotion of Science (JSPS).

REFERENCES

1. Fujisawa, H., Nagata, S., and Misono, H. (2003) Characterization of short-chain dehydrogenase/reductase homologues of *Escherichia coli* (YdfG) and *Saccharomyces cerevisiae* (YMR226C) *Biochim. Biophys. Acta.* **1645**, 89-94.
2. Kim, K-S., Pelton, J.G., Inwood, W.B., Andersen, U., Kutsyu, S., and Wemmer, D.E. (2010) The Rut pathway for pyrimidine degradation: novel chemistry and toxicity problems. *J. Bacteriol.* **192**, 4089-102.
3. Oppermann, U., Filling, C., Hult, M., Shafqat, N., Wu, X., Lindh, M., Shafqat, J., Nordling, E., Kallberg, Y. Persson, B., and Jornvall, H. (2003) Short-chain dehydrogenases/reductases (SDR): the 2002 update. *Chem. Biol. Interact*. **143-144**, 247–253.
4. Tanaka, N., Nonaka, T., Nakamura, K. T., and Hara, A. (2001) SDR: structure, mechanism of action, and substrate recognition. *Curr. Org. Chem.* **5**, 89–111.
5. Persson, B., Kallberg, Y., Oppermann, U., and Jörnvall, H. (2003) Coenzyme-based functional assignments of short-chain dehydrogenase/reductases (SDRs). *Chem. Biol. Interact.* **143-144**, 271–278.
6. Filling, C., Brendt, K. D., Benach, J., Knapp, S., Prozorovski, T., Nordling, E. Ladenstein, R., and Jörnvall, H., and Oppermann, U. (2002). Critical residues for structure and catalysis in short-chain dehydrogenases/reductases. *J. Biol. Chem*. **277**, 25677-25684.
7. Ito, K., Nakajima, Y., Ichihara E., Ogawa. K., Katayama, N., Nakashima, K., and Tadashi, Y. (2006) D-3-Hydroxybutyrate Dehydrogenase from *Pseudomonas fragi*: Molecular

Cloning of the Enzyme Gene and Crystal Structure of the Enzyme. *J. Mol. Biol*. **355**, 722−733.

8. Tanaka, N., Nonaka, T., Tanabe, T., Yoshimoto, T., Tsuru, D., and Mitsui, Y. (1996) Crystal structures of the binary and ternary complexes of 7α-hydroxysteroid dehydrogenase from *Escherichia coli*. *Biochemistry* **35**, 7715–7730.
9. Nakashima, K., Ito, K., Nakajima, Y., Yamazawa, R., Miyakawa, S., and Yoshimoto, T. (2009) Closed Complex of the D-3-Hydroxybutyrate Dehydrogenase Induced by an Enantiomeric Competitive Inhibitor. *J. Biochem*. **145**, 467-479.
10. Nakajima, Y., Ito, K., Ichihara, E., Ogawa, K., Egawa, T., Xu, Y., and Yoshimoto, T. (2005) Crystallization and preliminary X-ray characterization of D-3-hydroxybutyrate dehydrogenase from *Pseudomonas fragi*, *Acta Cryst. Sect F Struct. Biol. Cryst. Commun.* **61**, 36-38.
11. Tanaka, N., Nonaka, T., Yoshimoto, T., Tsuru D., and Mitsui, Y. (1996) Crystallization and preliminary X-ray crystallographic studies of 7α-hydroxysteroid dehydrogenase from Escherichia coli, *Acta Crystallogr. Sect, D Biol.Crystallogr.* **52**, 215-217.
12. Sambrook, J. and Russel, D. (2001). *Molecular cloning ; A Laboatory Manual,* 3rd edit Cold Spring Harbor Laboratory Press, Cold Spring Harbor
13. Otwinowski, Z. and Minor, W. (1997) Processing of X-ray diffraction data collected in oscillation mode. Methods Enzymol. **276**, 307–326
14. Collaborative Computational Project, Number 4 (1994) The CCP4 suite: programs for protein crystallography. *Acta Crystallogr. Sect D Biol. Crystallogr*. **50**, 760–763.

15. Brünger, A.T., Adams, P.D., Clore, G.M., Delano, W.L.,Gros, P., Grosse-Kunstleve, R.W., Jiang, J.-S., Kuszewski, J., Nilges, N., Pannu, N.S., Read, R.J., Rice, L.M., Simonson, T., and Warren, G.L. (1998) Crystallography and NMR system: a new software suite for macromolecular structure determination. *Acta Crystallogr. Sect D Biol. Crystallogr.* **54**, 905–921.

16. Emsley, P. and Cowtan, K. (2004) Coot: Model-building tools for molecular graphics. *Acta Crystallogr D Biol. Crystallogr*. **60**, 2126–2132.

17. Ke, S.H. and Madison, E.L. (1997) Rapid and efficient site-directed mutagenesis by single-tube 'megaprimer' PCR method. *Nucleic Acids Res*. **25**, 3371–3372.

18. Laskowski, R. A., Macarthur, M. W., Moss, D. S., and Thornton, J. M. (1993). PROCHEK: a program to check the stereochemical quality of protein structures. *J. Appl. Crystallogr.* **26**, 283-291.

19. Holm, L. and Rosenström, P. (2010) Dali server: conservation mapping in 3D. *Nucl. Acid Res.* **38**, 545-549.

20. Alasdair K. M., Nadia J. K., Helena H., Carol V. R., Christopher J. S., Christopher J. S., and Inger A. (2007) Clavulanic Acid Dehydrogenase: Structural and Biochemical Analysis of the Final Step in the Biosynthesis of the β-Lactamase Inhibitor Clavulanic Acid. *Biochemistry*. **46**, 1523-1533.

21. Prince, A. C., Zhang, Y. M., Rock C. O., and White S. W. (2004) Cofactor-induced conformational rearrangements establish a catalytically competent active site and a proton relay conduit in FabG. *Structure* **12**, 417-428.

22. Breton, R., Housset, D., Mazza, C., and Fontecilla-Camps, J. C. (1996) The structure of a complex of human 17beta-hydroxysteroid dehydrogenase with estradiol and NADP+ identifies two principal targets for the design of inhibitors. *Structure* **4**, 905-915.

23. Standley, D.M., Toh, H., and Nakamura, H. (2005) GASH: an improved algorithm formaximizing the number of equivalent residues between two protein structures. *BMC Bioinformatics* **6**, 221.

24. Kraulis, P. J. (1991) MOLSCRIPT: a program to produce both detailed and schematic plots of protein structures. *J. Appl. Crystallogr*. **26**. 283-291.

25. Fenn, T. D., Ring, D., and Petsko, G. A. (2003) POVScript^{+} : a program for model and data visualization using persistence of Vision ray-tracing. *J. Appl. Crystallogr.* **26**, 944-947.

TABLES

Table 1. Mutagenic and flanking primers

Primers	Nucleotide sequence
EcSDH1s	5’-CCGAATTCCATGATCGTTTTAGTAACTGG-3’
EcSDH2s	5’-CCCGGATCCATGATCGTTTTAGTAACTGG-3’
EcSDH2a	5’-CCCAAGCTTACTGACGGTGGACATTC-3’
EcSDH3s_Y141A	5’-CTGGCCGGCTGCCGGTGGTAACGTTTAC-3’
EcSDH4s_Y141F	5’-CTGGCCGTTTGCCGGTGGTAACGTTTAC-3’
EcSDH5s_F185A	5’-GGTACCGAGGCTTCCAATGTCC-3’
EcSDH6s_R189K	5’-CCAATGTCAAGTTTAAAGGC-3’
EcSDH7s_R189A	5’-CCAATGTCGCCTTTAAAGGC-3’
EcSDH8s_K151A	5’-GTGCGACGGCAGCGTTTGTTC-3’
EcSDH13s_F185L	5’-GGTACCGAGCTTTCCAATGTCC-3’
EcSDH14s_F185H	5’-GGTACCGAGCATTCCAATGTCC-3’
EcSDH15s_F185W	5’-GGTACCGAGTGGTCCAATGTCC-3’
EcSDH16a_R247A	5’-CCCAAGCTTACTGAGCGTGGACATTC-3’
EcSDH17a_R247K	5’-CCCAAGCTTACTGCTTGTGGACATTC-3’
EcSDH18a_ΔC7	5’-GGGAAGCTTAGGCATAGCTTTGG-3’
EcSDH19a_ΔC2	5’-CCCAAGCTTGTGGACATTCAGTCC-3’
EcSDH21a_ΔC1	5’-CCCAAGCTTAACGGTGGACATTC-3’
EcSDH23a_Q248N	5’-GGGAAGCTTAATTACGGTGGAC-3’
EcSDH24a_Q248A	5’-GGGAAGCTTACGCACGGTGGAC-3’

Mutagenesis codons are underlined.

Table 2 Data collection and refinement statistics

Serine dehydrogenase	Ligand-free enzyme		enzyme-$NADP^+$ complex	
Data collection				
space group	$P3_121$		$P6_4$	
cell parameters				
a (Å)	66.79		113.9	
b (Å)	66.79		113.9	
c (Å)	175.9		197.5	
wavelength (Å)	1.000		Cu*K*α	
resolution range (Å)	50-1.90	(1.93-1.90)	50-2.70	(2.75-2.70)
# of unique reflections	36,558	(1766)	39,711	(1991)
completeness (%)	99.7	(100)	99.8	(100)
redundancy	10.8	(11.0)	4.0	(4.0)
R_{merge}	0.073	(0.343)	0.126	(0.321)
mean I/σ (I)	37.5	(4.43)	12.4	(2.65)
Wilson B	58.8		47.0	
Refinement				
resolution range (Å)	20-1.90		20-2.70	
R-factor	0.200		0.194	
R_{free}	0.230		0.272	
average B-factors ($Å^2$)				
protein atoms	26.5		33.7	
water molecules	33.6		26.0	
$NADP^+$ molecules	-		32.5	
phosphate anions	-		63.7	
rms deviation				
bond lengths (Å)	0.005		0.007	
bond angle (°)	1.2		1.3	
Ramachandran plot				
most favored region	345	(92.5%)	1,133	(87.8%)
additional allowed region	28	(7.5%)	150	(11.6%)
generously allowed region	0	(0.0%)	7	(0.5%)

Values in parentheses refer to the outermost shell at the section of data collection.

Table 3 Kinetic parameters

Enzyme	L-serine			$NADP^+$		
	K_M (mM)	k_{cat} (sec^{-1})	k_{cat}/K_M (mM^{-1} sec^{-1})	K_M (mM)	k_{cat} (sec^{-1})	k_{cat}/K_M (mM^{-1} sec^{-1})
Wild-type	49	3.9	0.080	0.51	4.3	8.4
H_6-SerDH	29	2.4	0.083	0.70	3.0	4.3
Substrate recognition						
Y141A			no activity			
Y141F			no activity			
F185A			no activity			
F185L			no activity			
F185H			no activity			
F185W			no activity			
R189A			no activity			
R189K			no activity			
C-terminal region						
SerDH Δ C1	330	2.3	0.007	1.75	2.1	1.2
SerDH Δ C2			no activity			
SerDH Δ C7			no activity			
R247A	>500	–	–	–	–	–
R247K	127	2.0	0.016	1.4	3.1	2.2
Q248A	61	3.0	0.049	0.56	3.0	5.4
Q248N	62	2.3	0.037	0.47	2.4	5.1

FIGURE LEGENDS

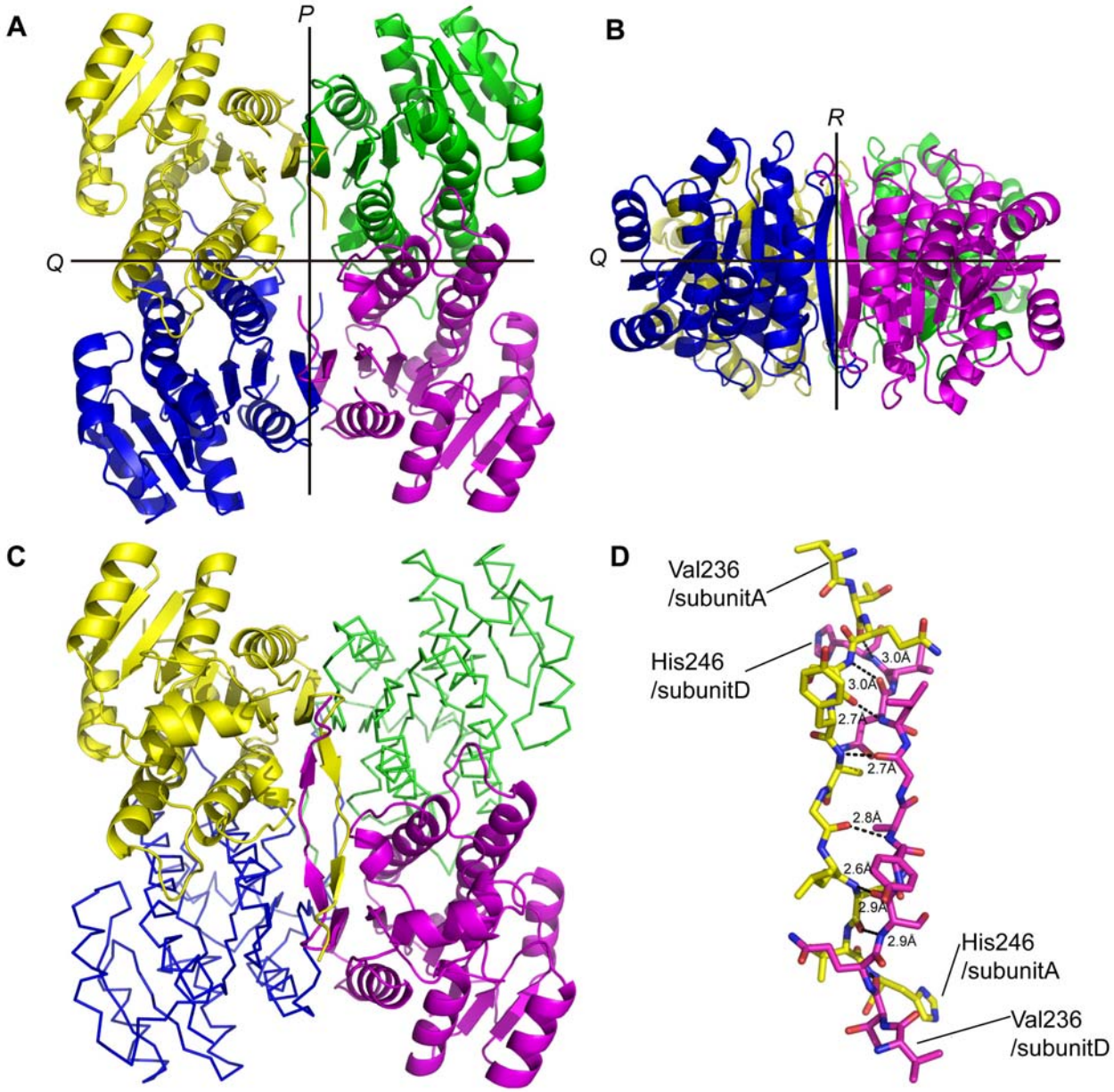

Fig. 1. Ribbon diagrams of SerDH.

The tetramers of the ligand-free enzyme are viewed along the *R*- (A) and *P*- (B) axes of non-crystallographic 2-fold axes consisting of 222 symmetry. Subunits A-D are represented by different colors: yellow, blue, light green and magenta, respectively. (C) The tetramer of the ternary complex with the same color as the ligand-free enzyme. A stretch of the C-terminal region forms antiparallel β-sheets with the same region of the opposite subunit each other. (D) A magnified view of the C-terminal β-sheets drawn as a stick model.

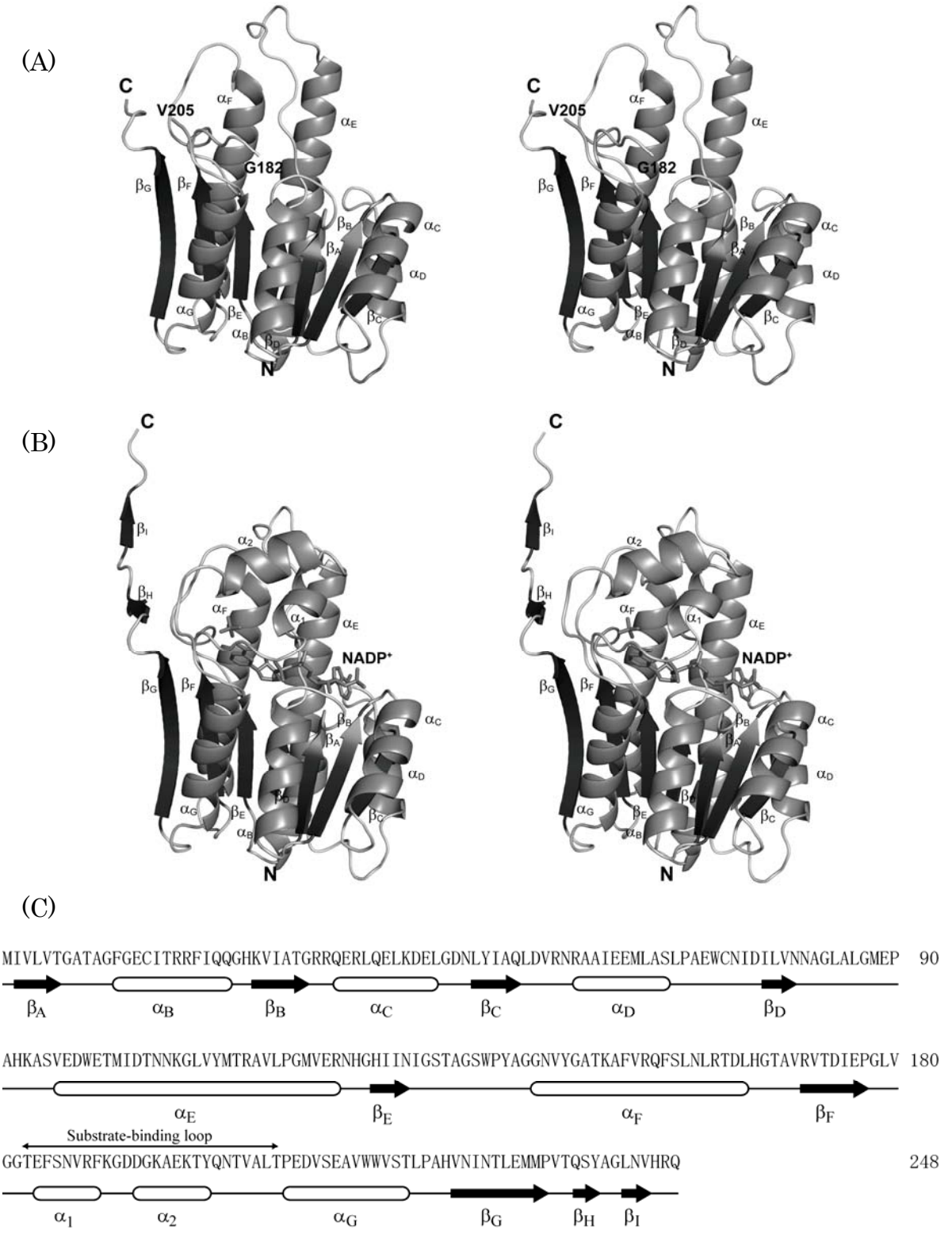

Fig. 2. Subunit structures of the ligand-free enzyme and the ternary complex.

Ribbon models indicate the ligand-free enzyme (A) and the ternary complex (B) with secondary structure assignments in stereo. The phosphate anion and $NADP^+$ are represented as stick models in dark and light gray, respectively. (C) Amino acid sequence of the SerDH. The secondary structure elements in the crystal structure are shown below the sequence.

(A)

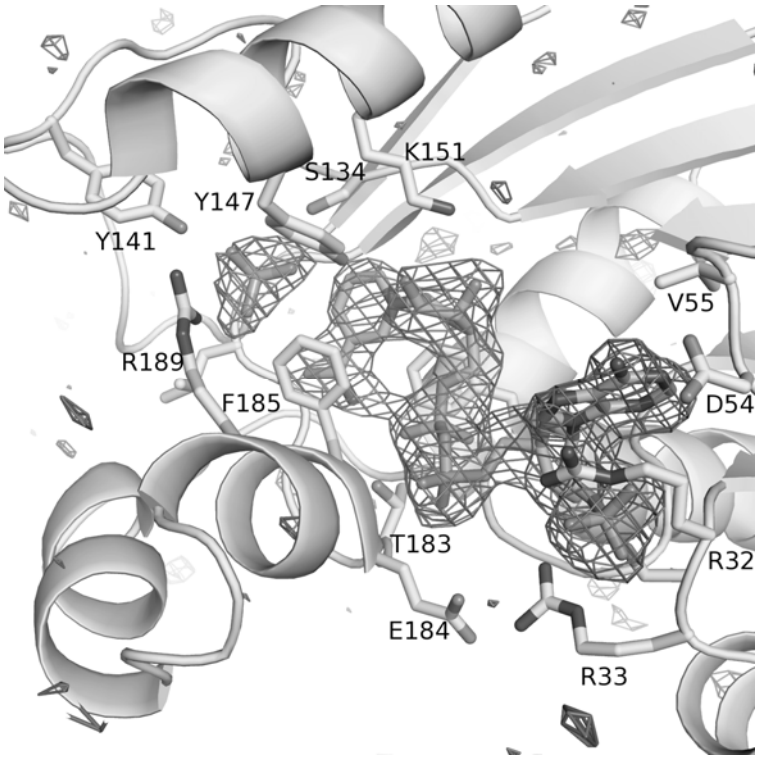

(B)

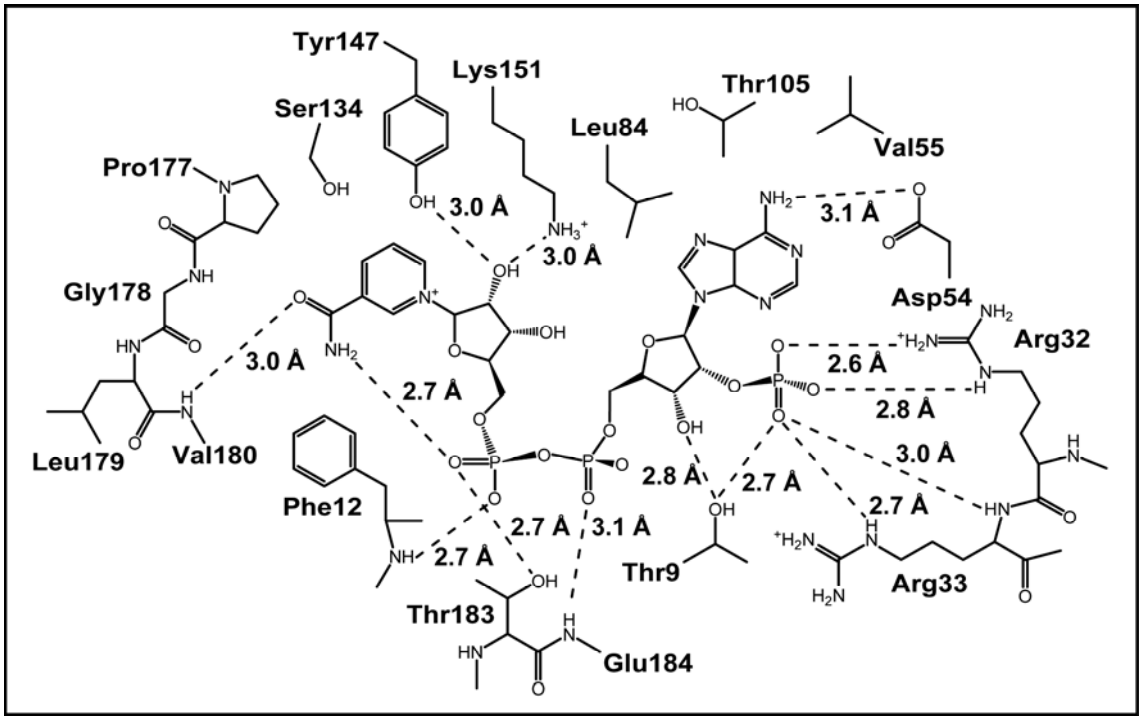

Fig. 3. Drawing of the $NADP^+$ binding site in SerDH.

(A) The wireframe shows the $F_O - F_C$ omit map for $NADP^+$ and phosphate anion contoured at 3σ levels. The stick models show residues interacting with $NADP^+$ or phosphate anion. (B) The scheme diagram shows hydrogen-bonding interaction with $NADP^+$ or phosphate anion.

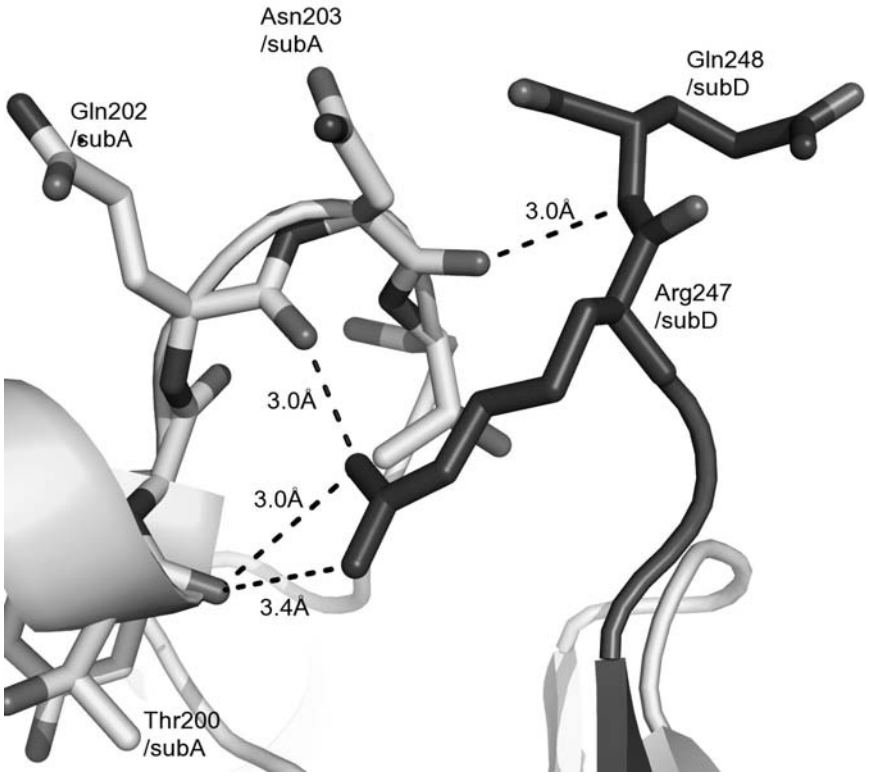

Fig. 4. Close-up view of interactions between the C-terminal region and the substrate-binding loop.

Subunits A and D are shown as light and dark gray, respectively. Arg247 and Gln248 on the C-terminal region in subunit A form hydrogen bonds with the substrate-binding loop in Subunit D.

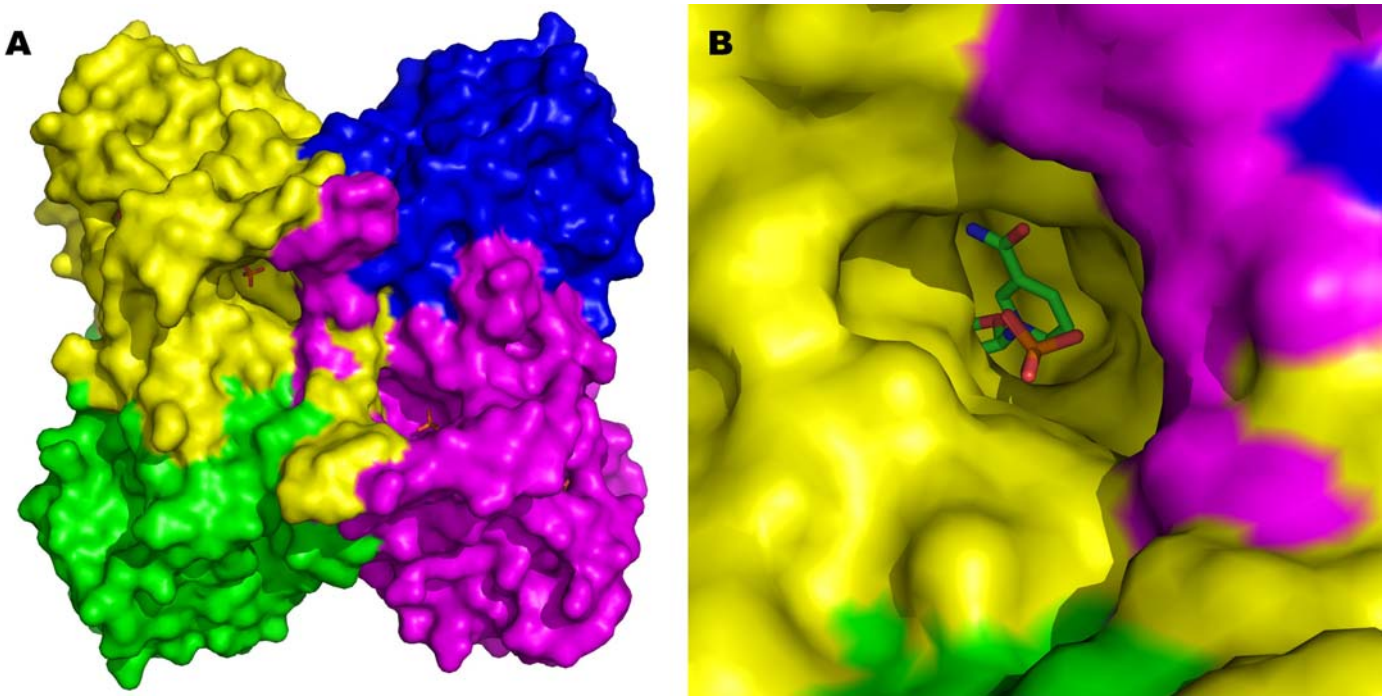

Fig. 5. Protein surface diagram of the ternary complex.

(A) Surface diagram of a tetramer. Surfaces of the subunits A, B, C and D in a tetramer are shown in yellow, blue, green and magenta, respectively. (B) Close-up view of the substrate binding pocket in subunit A. Phosphate anion and $NADP^+$ are shown as stick models. The active site of the SerDH is exposed to solvent.

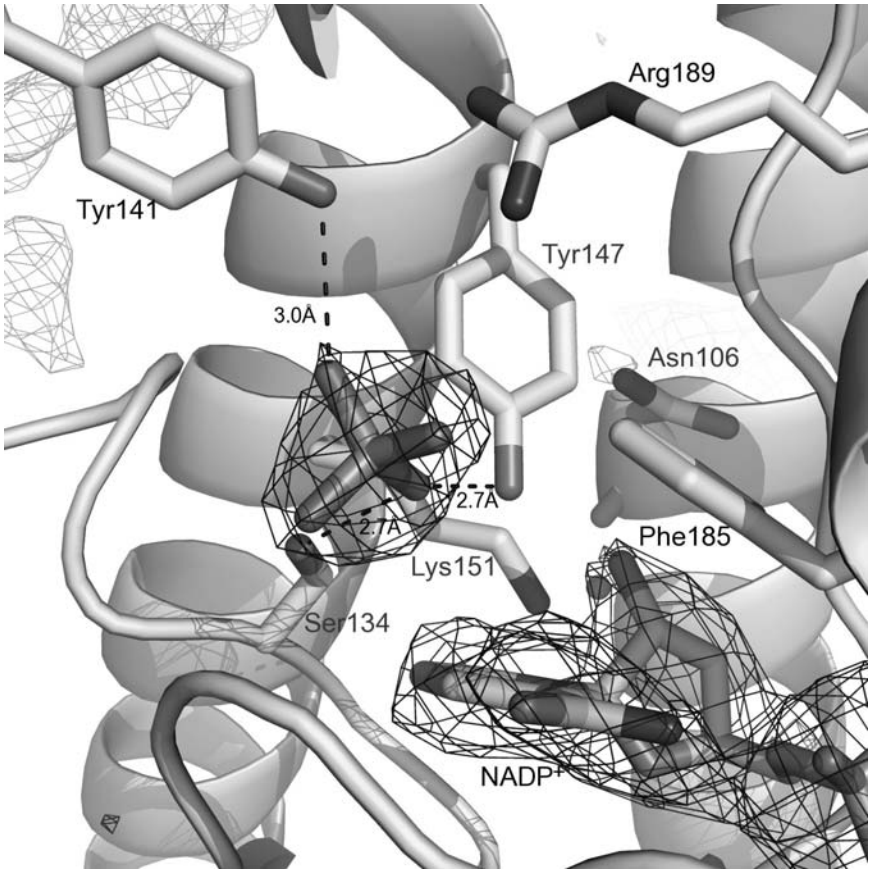

Fig. 6. The active site of the ternary complex.

The wireframe shows an $F_O - F_C$ omit map for $NADP^+$ and phosphate anion contoured at 3σ levels. The stick models show residues that are important for the catalytic reaction.

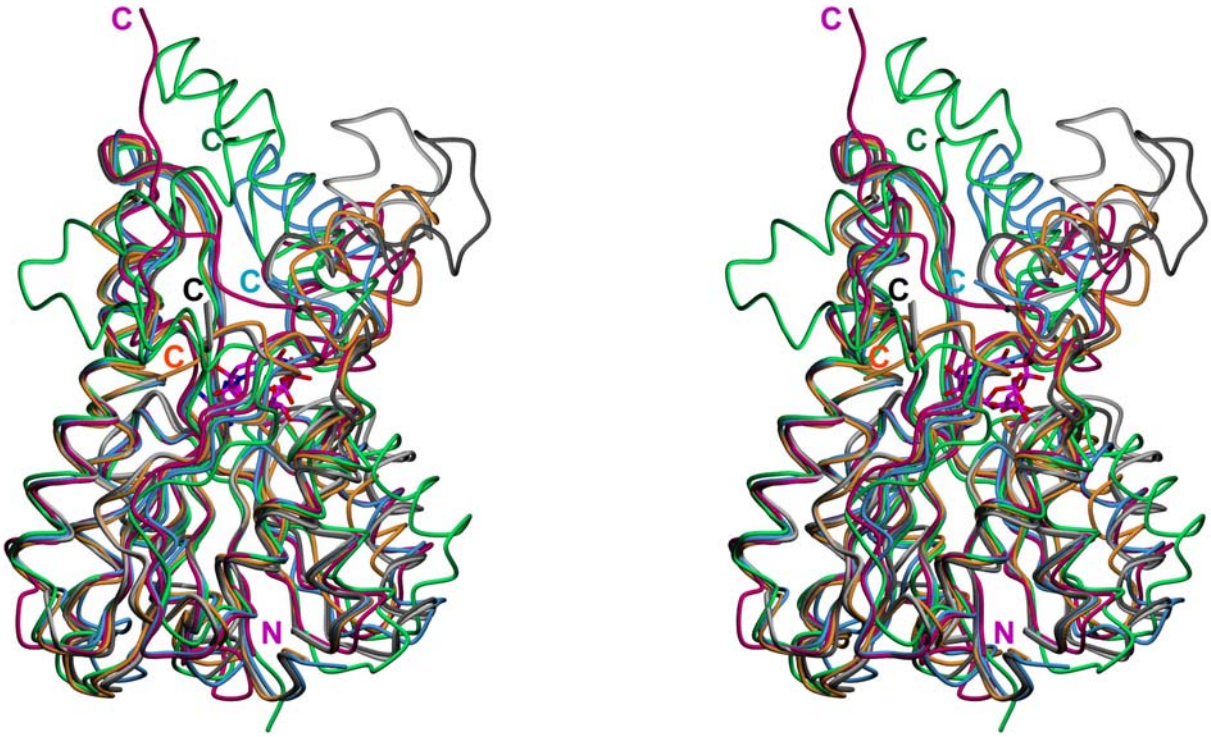

Fig. 7. Stereodiagram of superimposition among the ternary complex and SDR enzymes.

The main chain of the ternary complex is represented as a magenta line, and those of CAD (2JAP), FabG (1Q7B), 17β-HSDH (1FDT), and PfHBDH with open and closed forms (1WMB and 2ZTL) are shown in sky blue, orange, light green, dark gray, and light gray lines, respectively. The N-terminal of the ternary complex and the C-terminal of each enzyme are indicated as letters in the same color. A stick model indicates the $NADP^+$ in the ternary complex. This diagram is drawn and rendered by the programs $POVscript^+$ (*24*, *25*) and POVray (http://www.povray.org), respectively.

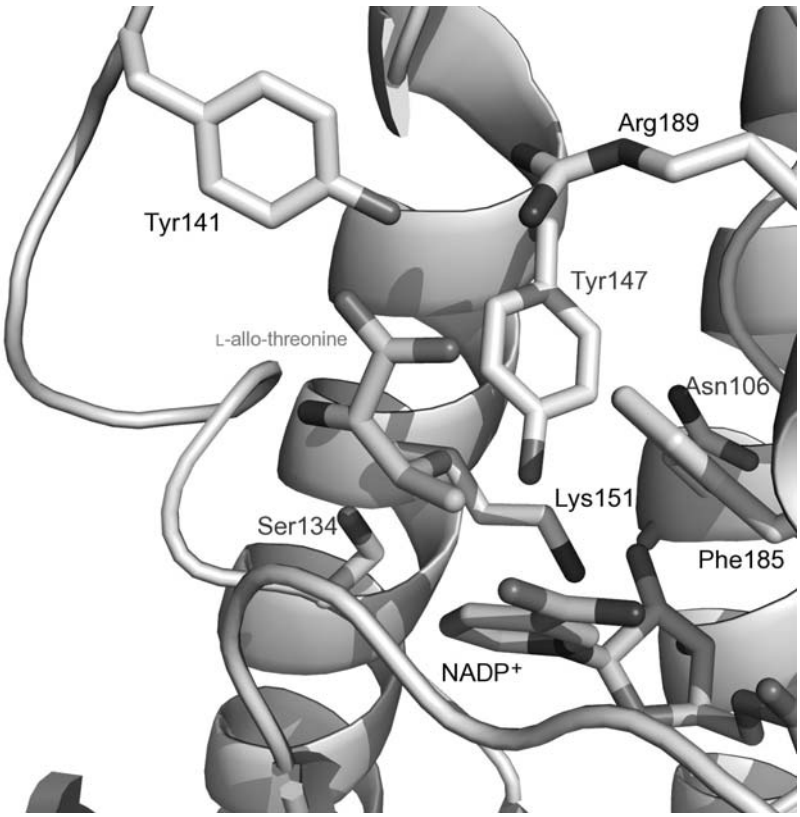

Fig. 8. Simulated model of the SerDH complexed with L-allo-threonine.

Residues, L-allo-threonine, and $NADP^+$ at the active site are represented as stick models.